IET Generation, Transmission & Distribution

The Application of Let-Through Energy to Back-up Over-Current Protection on High Voltage Feeders

GTD-2018-6190 | Research Article

Submitted by: R. C. Bansal, Martin Slabbert, Raj Naidoo

Keywords: POWER SYSTEM PROTECTION, RADIAL DISTRIBUTION FEEDER, HIGH VOLTAGE TRANSMISSION LINES, PROTECTION ALGORITHM, THERMAL PROTECTION, OVERCURRENT PROTECTION

The Application of Let-Through Energy to Back-up Over-Current Protection on High Voltage Feeders

Martin J. Slabbert [1], Ramesh C. Bansal [2*], Raj Naidoo [2]

[1] Transmission System Operator, Eskom, Johannesburg, South Africa.
[2] Department of Electrical, Electronics and Computer Engineering, University of Pretoria, Pretoria, South Africa.
[*] rcbansal@ieee.org

Abstract: Let-through energy (LTE) refers to the I^2t or Joule energy that a conductor is exposed too during a fault on the feeder. This energy is influenced by the magnitude of the fault current and time it takes for the protection system to clear the fault. If the LTE exceeds the conductor thermal energy limit, the conductor will get damaged. This concept of LTE evaluation is applied to the inverse definite minimum time (IDMT) current based back-up protection elements on a multisource high voltage feeder in a hypothetical and actual network. Another method to calculate the relay operating time for IDMT relays was developed based on an average disk speed of electromechanical over-current relay and the proportionality of its speed to the magnitude of the fault current. This method was incorporated into a software application to generate results. These results allow the user to evaluate the conductor LTE exposure, total fault time exposure, the effect of instantaneous fault clearing and the application of auto-reclose cycles. An energy-area evaluation was applied to quantify and evaluate small protection settings changes. The conclusion is that LTE analysis on back-up protection should be considered for high voltage feeders to ensure that the conductors are protected.

1. Introduction

High voltage (HV) feeder protection schemes normally consist of main and backup protection relays. High voltage is defined by the IEEE as a voltage ranging from 1 kV (including) up to a voltage of 100 kV (less than) [1]. In South Africa this is extended up to 132 kV (including) [2]. Main protection relays make use of impedance, differential or pilot protection to protect HV feeders [3]. Over-current based protection relays are used to provide backup protection to the main protection relays [3-6]. This back-up protection is for both phase and earth faults [6]. Current based back-up protection is an uncomplicated element and relatively inexpensive to apply [5-9]. However, it can be difficult to set because of its simplicity (selectivity for complex networks and long operating times) [7, 9, 10]. Generally, current based protection consists of an instantaneous element and a time delayed element [10]. When setting the time delayed over-current elements, the sensitivity of the pickup, the speed of operation and selectivity of the element are considered [11]. The relay operating time should be kept to a minimum [11]. However, the time delayed element is set slower than the main protection elements [3, 5]. It also requires coordination studies to ensure selectivity with other time delayed elements, but this coordination requirement increases the fault clearing time [3].

Over-current relays are used to perform over-current and not overload protection [3]. With main protection applied to HV feeders, little attention is given to ensure that the backup protection is actually protecting the feeder. A focus is placed on setting the protection insensitive to load current and sensitive to fault current [3-5, 8-12]. This does not mean that the actual conductor is protected. Conductor protection can be achieved by considering a damage curve based on the conductor annealing [7, 8]. The heat required for the conductor material to anneal is generated from the flow of fault current. The application of let-through energy (LTE) protection to radial medium voltage (MV) feeders was developed in [13]. For a radial feeder it is simply the fault current, exposure time and the number auto-reclose (ARC) attempts that influence the LTE. When applying this concept to a feeder consisting of more than one supply point the complexity of calculating the conductor LTE exposure increase due to the measured root mean squared (RMS) fault current changing with every circuit breaker (CB) operation in an interconnected network, the protection settings for the overcurrent elements being different at each end of the feeder and more than one CB operation is required to clear the fault.

The application of current based backup relays to HV feeders are not new. The application of let-through energy analysis to a network consisting of more than one point of supply is new, thus considering the power system with the applied protection philosophy and not just the specific position in the system. The analysis is done on HV feeders, but it is very applicable to new generation medium voltage smart grids where there is only current based protection with multiple supply points in one feeder. In this article we have shown how to calculate conductor limits, create conductor damage curves and then why we need to consider LTE protection for HV feeders. To apply the LTE concept to a multisource feeder a new over current relay model was developed and a software application generated. The software application was applied on two hypothetical multisource feeders and an actual feeder to illustrate the concept of evaluating LTE in a multisource network that use current based relays.

2. Let-through energy

LTE refers to the amount of I^2t energy (fault current and clearing time) that the conductor is exposed to during a fault. This is also called a Joule integral or specific energy [14, 15]. This time should include breaker operating time,

arcing time and the coordination time (relay trip time based on operating curve and settings) [15]. The fault current will heat the conductor and cause the conductor to sag. Once the fault is cleared by the protection system, the conductor should return to its original position when it is cooled down. This is termed an elastic deformation cycle and occurs if the stress and strain changes on the conductor material is proportional [16]. However, if the conductor is heated to such an extent that the stress on the conductor is beyond its proportional limit, plastic deformation will occur. This means that the conductor will sag initially (due to heating effect from fault current) and once the conductor temperature is reduced, it will not return to its original profile. Thus the conductor is damaged. The conductor will still be in service, but the conductor metal is deformed and this will cause a failure in time [8].

2.1. The conductor limit

The conductor damage curve (annealing) is an I^2t curve [8, 11, 17]. The maximum current that the some conductor types can sustain for 1 s (without getting damaged) is show in Table 1 [18]. Table 1 also shows the associated I^2t limit or LTE limit. The LTE limit of a conductor can be calculated using (1) [17].

Table 1 Conductor current and energy limit

Conductor Type	Fault current for 1 s (kA)	I^2t Energy (MA^2s)
Chickadee	17.17	294.81
Hare	8.97	80.46
Kingbird	27.58	760.66
Mink	5.40	29.16
Oak	9.59	91.97
Tern	39.36	1549.21
Bear (calculated)	26.29	691.16
Wolf (calculated)	15.72	247.12

Equation (1) is derived by setting the electrical energy equal to the heat energy absorbed in the conductor [17, 19-21]. This can be done when the assumption is made that it is an adiabatic process [14, 20, 21]. The heat energy generated (Joule) is equal to the resistance of the conductor, times the square of the current and this then multiplied with the time the conductor is exposed to this current [17, 22].

$$I^2R \cdot t = \left(\frac{W \cdot S \cdot 10^3}{\alpha}\right) \log_e\left(1 + \alpha(T_2 - T_1)\right) \quad (1)$$

Where I is the fault current (kA), t is the fault duration (s), W is the mass of the conducting material (kg/km), S is the heat capacity of the conducting material (J/°C·g), R is the resistance of the conductor at T_1 (Ω/km), α is the temperature coefficient of resistance (per °C), T_1 is the conductor temperature before the fault (°C) and T_2 is the conductor temperature after the fault (°C).

A pre-fault conductor temperature of 75 °C was used in [18] and a value of 50 °C was used in [17]. The conductor prefault or initial temperature (T_1) should be chosen equal to the maximum operating temperature of the conductor [14]. A final temperature of 200 °C is recommended [14, 17, 18]. The 1 s fault current capability of Wolf and Bear conductors were calculated using (1) with initial and final temperature values of 75 °C and 200 °C respectively (results added to Table 1).

2.2. Damage curves and let-through energy exposure

The I^2t energy level in Table 1 is the damage curve for the respective conductor (horizontal straight line in terms of LTE) [13]. The resulting LTE exposure due to the over-current protection should be less than the conductor damage curve (energy level) to ensure it is protected [7, 8, 12, 14, 19, 20].

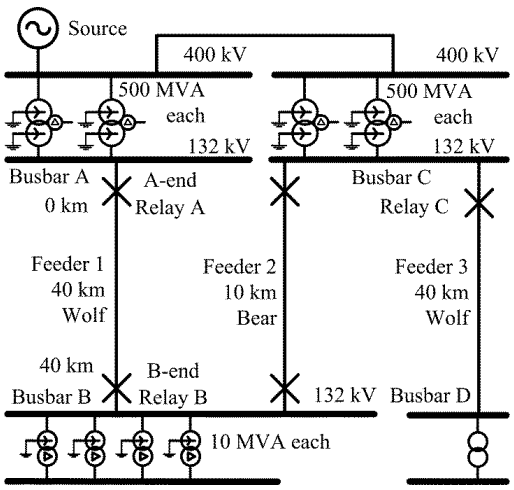

Fig. 1. *A network consisting of an interconnected section and a radial HV feeder (Feeder 3) is shown.*

In the network diagram of Fig. 1 there is an interconnected network section by means of Feeder 1 and 2. Feeder 3 is a radial feeder from Busbar C. The IEC normal inverse (NI), inverse definite minimum time (IDMT) relay equation of (2) can be used to calculate the expected operating time of a relay for a specific constant RMS current [10, 23].

$$OT = \frac{0.14 \cdot TM}{\left(\frac{If}{Ipu}\right)^{0.02} - 1} \quad (2)$$

Where OT is the operating time of the protection element (s), TM is the time multiplier (unit less), If is the fault current (A) and Ipu is the pick-up current (A).

By increasing the time multiplier (TM), the relay operating time will increase. The operating time will also increase as the ratio of fault current to pick-up current in (2) becomes smaller (further away from the source). The conductor LTE exposure is calculated by multiplying the square of the fault current with the fault clearing time [13]. As this is done across the length of the feeder, a LTE curve is generated.

For a radial feeder the LTE tends to decrease from the source busbar towards the load busbar (e.g. Busbar C towards Busbar D in Fig. 1). Close to the source the LTE

level is high and is dominated by the fault current [11, 13]. At a certain point on the feeder the time component of the I^2t equation will become dominant and there will be an increase in the LTE exposure. This increase is as a result of the fault level to pick-up ratio approaching a value of 1 [9]. It is thus possible to have a LTE peak or exceedance at both ends of the feeder. With a small change in the protection settings the LTE peak at the end of the feeder can be reduced. The initial LTE peak due to fault current being dominant requires settings changes or a reconfiguration of the network to reduce the fault current magnitude.

2.3. *The effect of an auto-reclose cycle on the energy exposure*

By applying the ARC function, the network availability can be improved by restoring supply for transient faults automatically [4, 10, 24]. In contrast to this, exposure of the source transformers to another through fault due to an ARC cycle (if permanent) will reduce the life expectancy of the transformers [24]. If the back-up protection is allowed to trip for a second time (1 ARC cycle), then the conductor will be exposed to the same fault current and exposure time again. This cumulative exposure for all ARC cycles was also considered in [13] and [21]. The accumulation is under the assumption that no heat energy is lost to the surrounding environment during the ARC dead time. For a radial feeder the total LTE can be calculated by multiplying the square of the fault current with the total fault time exposure to a fault (include every ARC attempt) at that specific point on the feeder [13]. When one ARC cycle is applied not only does the energy level increase close to the source but the high LTE levels will also penetrate further into the feeder. This is further down from Busbar C to Busbar D on Feeder 3 in Fig. 1. The potential for damaging this conductor thus also increase. The choice of ARC philosophy impacts the choice of conductor to be used or one can also argue that the choice of conductor influences the ability to ARC.

For an interconnected or multisource network, the fault current will change when a CB changes state. To calculate the total LTE at that position on the feeder, the sum of the LTE of each current magnitude for a specific duration have to be added together until the fault is cleared and all ARC cycles from all breakers supplying the fault are depleted. For a radial feeder it was simply the fault current magnitude multiplied with the fault clearing time and the number of ARC cycles. For multisource feeders, an increase in the LTE at the remote end can be a combination of the remote end (Busbar D end) and the local end (Busbar C end) LTE contribution.

3. Motivation for application on HV feeders

Eskom is the primary electricity utility in South-Africa responsible for generating, transmitting and distributing electricity to a multitude of domestic and international customers [25]. Based on the annual fault level report a histogram (Fig. 2) was created for the 132 kV Transmission busbar fault levels in the Eskom grid [26].

In Fig. 2 it is observed that the fault levels range from 5 kA to 45 kA. The 50th and 80th percentile of the three phase fault currents in Fig. 2 are 16.89 kA and 25.24 kA respectively. The average three phase fault current is 15.68 kA with a standard deviation of 7.67 kA. The average fault current is close to the 50th percentile current. If the average current was used to determine if LTE protection should be applied, it will only cover 50 % of all the busbars. Thus the 80th percentile is used for this evaluation. The busbar fault level includes the feeder under study's own contribution to the busbar fault level. The 80th percentile for single phase to ground faults is 21.88 kA.

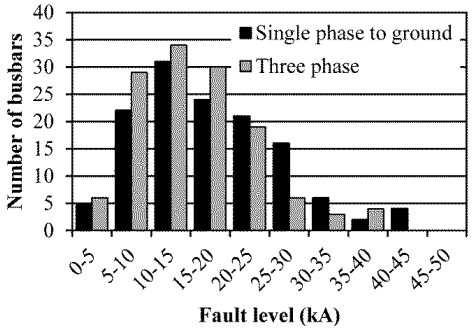

Fig. 2. *The single-phase-to-ground and three-phase fault level distribution at 132 kV Eskom transmission substation busbars.*

Table 2 Conductor fault current withstand time

Conductor	Single phase to ground fault withstand time at 80th percentile (s)	Three phase fault withstand time at 80th percentile (s)
Chickadee	0.497	0.662
Hare	0.158	0.21
Kingbird	1.287	1.712
Mink	0.057	0.076
Oak	0.143	0.19
Tern	2.034	2.707
Bear	1.085	1.444
Wolf	0.388	0.516

By using (3) and the 1 s fault current values in Table 1 the new fault current withstand time for a conductor can be calculated [13]. This is done for the conductors of Table 1 at the various percentiles of fault current and the results are shown in Table 2. From the withstand times that are calculated in Table 2 it can be seen that many of the conductors have very small exposure time limits at the 80th percentile. This analysis does indicate that LTE protection should be evaluated at HV voltage levels to ensure the conductors are protected.

$$t_{new} = \left(\frac{I_1}{I_2}\right)^2 t_{old} \quad (3)$$

Where t_{new} is the new fault withstand time (s) at I_2 fault current (A) and t_{old} is the previous fault withstand time (s) at I_1 fault current (A).

4. Multi-source feeder applications

Feeder 1 in Fig. 1 consists of a CB with a protection relay (and independent settings) on both ends of the feeder as this is an interconnected network (supply from both ends).

For a fault on the feeder plasma will form at the fault position [27-29]. Within the plasma there will be streamers [28, 29]. These streamers will tend to move away from the feeder fault position in the direction of the arc. The conductor will experience the fault current from Busbar A up to the fault point and on the other side it will experience the fault current from Busbar B up to the fault point.

4.1. Feeder circuit breaker operating sequence

Fault current distribution in an interconnected network will change when a CB operates and this has an effect on the operating time of the IDMT over-current protection elements. There are many possible network conditions that exist based on the change in fault levels, the protection settings and protection philosophy that are applied to the feeder. Two possible sequences of events are illustrated in Fig. 3 when a fault occurs on the feeder with one ARC cycle applied.

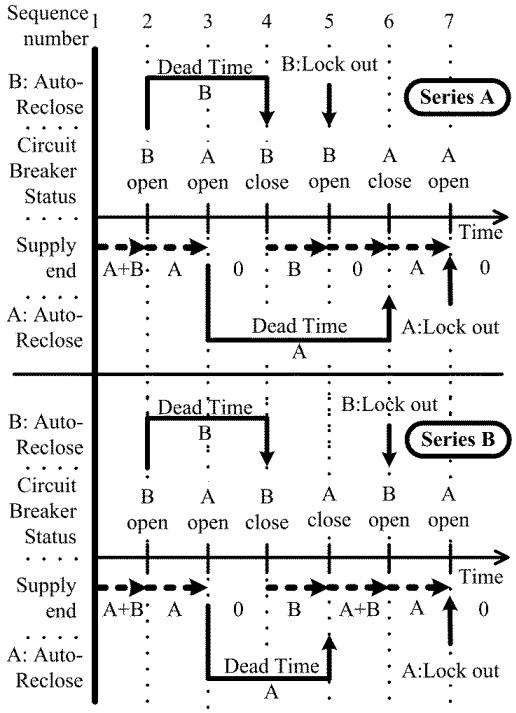

Fig. 3. *Two possible sequences of event diagrams indicating the ARC state, the status of each breaker and which end of the feeder is feeding the fault.*

The following sequence of events discussion is with reference to Series A in Fig. 3. In this application the protection relay's reset curve is set to reset instantaneously. A permanent fault is placed on the feeder at sequence event number 1. Initially the fault current is supplied from both A and B sides of the feeder. In this case the B-end is opened first and fault current is now only supplied from the A-end of the feeder (event 2). When the trip signal is sent to the CB, the dead time timer on the B-end relay is also started [10, 24]. The fault current that relay-A is experiencing is changed when the B-end is opened. After a certain time (based on protection settings) the A-end relay will open the CB and it will start the dead time timer on this end (event 3). During this period no current will be supplied to the fault. This is to allow the ionized air to disperse, the breaker mechanisms to reset and relays to reset if required [4, 10, 24]. If the B-end dead time was not long enough, the breaker at the B-end will close before the A-end has opened, thus the fault will not be isolated on the first ARC attempt. If the dead time was long enough, the feeder will be energized from the B-end (event 4).

Depending on the settings that are applied to the B-end, the CB can trip before the A-end closes, thus creating another period where the feeder is isolated. If this was not the case, it will resemble the sequence of Series B in Fig. 3 where the A-end will also close and the fault will be supplied from both ends of the feeder (event 5, Series B). Every time there is a CB operation, the fault current distribution will change. Once the B-end has tripped a second time (one ARC cycle) it will reach its lock-out state where it will not initiate another CB close (event 5, Series A). When the A-end close (event 6, Series A), it will now supply the fault current and eventually trip and go into lock-out (event 7). The feeder will now remain de-energised for the permanent fault. From the two sequence diagrams in Fig. 3, it can be seen that the protection settings will influence the LTE exposure of the feeder.

4.2. Over-current relay model

For the radial networks considered in [13] the NI IDMT equation of (2) is adequate to calculate the relay operating time. In an interconnected or multi-source network the CB's at different positions can operate at different times to isolate the same fault. The measured RMS fault current through the relay can change, and this will change the operating time of the over-current relay [22, 30]. If the RMS current change over time, (2) cannot be used in this form. The integral form of (4) can be used to calculate the relay operating time, but the RMS fault current signal should be defined so as to compute the integral. This RMS current signal is not known before the fault. Equation (4) is a simplification of the full induction disc relay (electromechanical) operating equation [23, 30-32]. One of the simplifications is that the inertia of the disc is neglected [6, 31-33]. If there is discrete sampling of the current waveform, the trip time can be determined by adding each time step (area under the curve) together and determining the time required for it to equal 1 (as in (4)). For this approach the complete RMS fault current signal is not required beforehand. This is with *t(I)* equal to (2). On an actual relay, this is implemented by numeric integration based on the current sampled values during specific time steps [30].

$$1 = \int_0^{T1} \frac{1}{t(I)} dt + \int_{T1}^{T2} \frac{1}{t(I)} dt \qquad (4)$$

Where *T1* is the end of the first event time (s), *T2* is the end of the second event time (s) and *t(I)* is the time current characteristic equation.

The over-current relay used in this work was modelled on the assumption that the disk speed is constant if

the RMS current is constant and the inertia of the disk can be ignored. With these assumptions the time required for the disk to move from the start to the trip position can be calculated using (2) for a constant RMS current. The TM is proportional to the angular distance that the disk has to travel. Using the trip time for a constant current and distance the disc needs to travel (set equal to the TM value) an average linear disc speed can be calculated. Every time the current change, a new disk speed, the distance that the disk has travelled and then still require to travel for a trip can be calculated. From this the total trip time is then determined for a variable current signal. This approach is valid for both electromechanical and numeric relays.

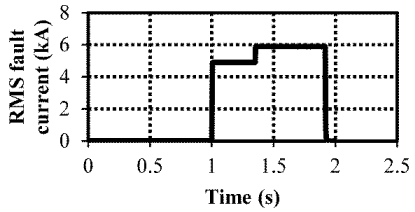

Fig. 4. *The RMS fault current results from the simulation software.*

An example of this average speed relay model approach is shown for the root mean square (RMS) fault current signal in Fig. 4. A fault was applied to the feeder at 1 s and then at 1.35 s another source was switched in to increase the fault current from 4892 A to 5883 A. A similar fault current input was used in [22]. For the simulation a TM of 0.31 and pick-up current of 550 A was applied to a NI IDMT element on the relay. If the current stayed constant at 4892 A, it would result in a trip time of 0.971 s and if the current was equal to 5883 A the trip time would have been 0.894 s. In the simulation the feeder was exposed to this fault current and the current was interrupted at 1.92 s. The fault duration was thus 0.92 s. By applying the average disk speed relay model the resulting trip time equals 0.922 s.

This average speed over-current relay model was verified by means of calculating the operating time using (4) and by means of simulation in power system simulation software. Both methods indicate the average disc speed method is adequate for this work.

A software based application was created to evaluate the LTE that a feeder will be exposed too. This application made use of the average disc speed over-current relay model and incorporated the complex sequencing as shown in Fig. 3.

5. Results

Results were generated for two network conditions on Feeder 1 in the HV network of Fig. 1. The settings that are applied to each end of the feeder in all three case studies are shown in Table 3. In the first case study the fault levels at Busbar A is high (20 kA) when compared to Busbar B (8.7 kA). In the second case study the network is changed so that the fault levels at Busbar A (20 kA) and Busbar B (18 kA) is almost the same. For the third case study the concept was applied to a feeder in an actual network. All of these results were generated using three phase fault levels. The measured fault current (at relay A or B) will change when a CB is opened in the interconnected network. A CB operating time of 50 ms is applied to all the instantaneous curves.

Table 3 Applied settings for different case studies

Case Study	*Feeder End*	*Curve*	*Pick-up (A)*	*TM*	*Instantaneous pickup (A)*
1	A-end	Normal inverse	630	0.41	10000
1	B-end	Normal inverse	630	0.1	4500
2	A-end	Normal inverse	630	0.41	10000
2	B-end	Normal inverse	630	0.4	10000
3	A-end	Normal inverse	600	0.2	None
3	B-end	Normal inverse	600	0.375	9000

5.1. Case study 1- High and low fault levels

For case study 1 the B-end is set to trip faster than the A-end. One ARC cycle (3 s dead time) and an instantaneous over-current element can be applied to both ends of the feeder.

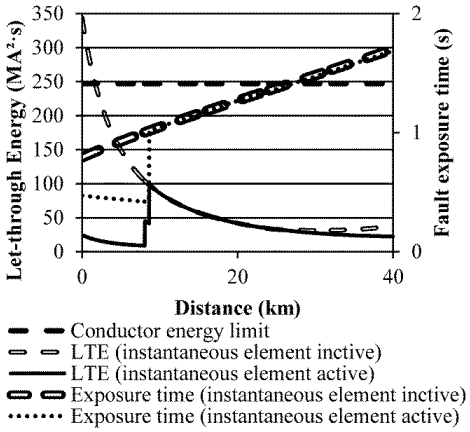

Fig. 5. *The LTE and fault exposure time on the feeder based on the three phase fault levels and the protection settings in Table 3 (No ARC).*

The total LTE and fault exposure times are shown in Fig. 5 for when the instantaneous element is active and inactive. No ARC cycles are applied for the results in Fig 5. The conductor I^2t energy limit does not change and hence we have the horizontal line at 247 $MA^2{\cdot}s$ for Wolf conductor. First, consider the LTE curve with the instantaneous element inactive. The conductor can get damaged due to the thermal effect of the fault current within the first 1.5 km from Busbar A. The LTE will then reduce to a minimum at 34 km's and increases again slightly. The initial LTE peak is dominated by the fault current, with the fault duration at its minimum close to Busbar A (roughly 0.8 s). For faults towards the end of this feeder, the conductor is less likely to get damaged, but other equipment that is exposed to the long duration fault current they must carry such as the transformers at Busbar A can get damaged. This is more mechanical damage than thermal damage for a transformer [34].

On longer feeders the effect of time can become dominant as the ratio of fault level to pick-up current

approaches one. The pick-up current, TM setting, network state (plant in service), the type of fault, fault position and fault resistance all have an influence on the plant LTE exposure. The area under the LTE curve is determined and used to quantify the effect of settings changes [13]. For the LTE (instantaneous element inactive) curve of Fig. 5, the energy-area calculates 2973.7 MA²·s·km.

An instantaneous element can be used to reduce the fault clearing time for a fault close to the source or busbar of the feeder [4, 9, 10]. This reduction in trip time will reduce the damage at the fault location [10]. The LTE (instantaneous element active) curve in Fig 5 shows the initial conductor energy exceedance is now removed and the energy peak is now moved further down the feeder (8.5 km's from Busbar A). This is now the area where faults will most likely result in conductor thermal damage.

There is a small change in the energy curve 8.5 km from Busbar A as the operating time transitions from the instantaneous curve to the IDMT curve. The change occur at the 50 MA²·s energy level (8.5 km) and is due to the fault levels that are changing as different CB's operate. The protection will operate on a different curve again for a small portion (distance) of the feeder. The fault exposure time close towards Busbar A was reduced by the instantaneous element but the maximum time (40 km from Busbar A) did not show significant change. This lack of change indicates that it was dominated by the fault current and protection settings at the A-end of the feeder. Even though the instantaneous element was activated at the B-end, the effect was similar to the IDMT element that was already applied. For the LTE (instantaneous element active) curve, the energy-area calculates to 1443.1 MA²·s·km. This shows that the energy-area exposure was halved by applying the two instantaneous elements. If the instantaneous element at the B-end was disabled, the energy-area would increase slightly to 1540.9 MA²·s·km. This confirms that the effect of the instantaneous element at the B-end of the feeder is almost negligible.

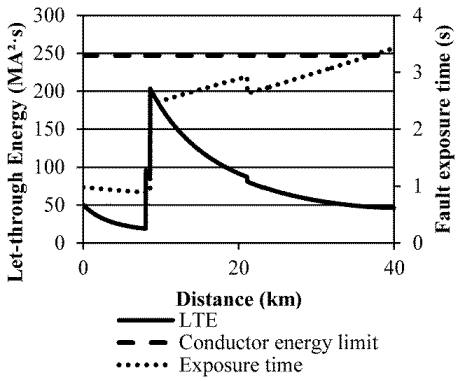

Fig. 6. *The LTE and fault exposure time on the feeder based on the three phase fault levels and the protection settings in Table 3 with the instantaneous elements active and one ARC applied to both ends of the feeder.*

For the results in Fig. 6 one ARC cycle is applied to both ends of the feeder with the IDMT and instantaneous elements still active. The peak LTE position did not change on the feeder as the instantaneous element settings did not change. However, the magnitude of this energy is doubled. The energy exposure time also doubled with the maximum time still at the end of the feeder. There is now a step change in the fault exposure time curve (at 20.6 km) due to the sequence of events where different ends can supply the fault at different times. For the LTE curve of Fig. 6, the energy-area calculates 3007.3 MA²·s·km. If the instantaneous elements was removed, the energy-area would increase to 6220.5 MA²s·km. This emphasizes fast fault clearance close to the high current source end.

5.2. Case study 2 – High fault levels at both ends of the feeder

For case study 2, the fault level at Busbar B is increased on a similar network to that of Fig. 1. The results in Fig. 7 are shown with both instantaneous elements active and both ends have been set to initiate one ARC cycle (dead time of 3 s). In this case study the conductor energy limit was not exceeded if the instantaneous elements are active. If the instantaneous element at the remote end is inactive it can be seen that the conductor limit will be exceeded 33.8 km from Busbar A towards Busbar B. The fault exposure time also increases further down the feeder (instantaneous element inactive) and this is now a high fault current region with slow operating times which can damage equipment such as transformers (damage is cumulative) [24].

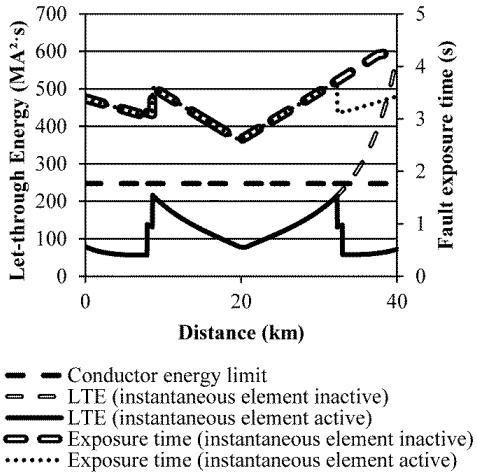

Fig. 7. *The LTE and fault exposure time on the feeder based on the three phase fault levels and the protection settings in Table 3.*

With both instantaneous elements active, there are now two energy peaks at positions on the feeder where there is a transition from fast instantaneous operating curves to slow IDMT operating curves. The fault exposure time is ranging in a fairly horizontal band for this scenario. The energy-area calculation results in a value of 4297.9 MA²·s·km which is an increase to that of case study 1, but it is still less than the value when the instantaneous element is inactive in case study 1. If the

instantaneous element on the remote end was removed, the resulting energy-area calculates to 6465.3 MA²s·km. This shows that the instantaneous element has a significant impact on energy exposure when fault levels are high.

5.3. *Case study 3 – Actual feeder evaluation*

In case study 3 an actual HV feeder in the Eskom HV network was used. The network resembles that of a 100 km feeder (Wolf conductor) with a point of supply from both ends. The fault level at Busbar A is 4.7 kA and Busbar B it is 24.5 kA. The backup OC element is not set to initiate ARC.

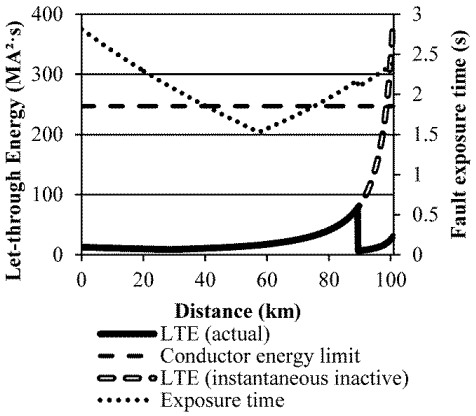

Fig. 8. *The LTE and fault exposure time on an actual feeder based on the three phase fault levels and the protection settings in Table 3.*

The LTE results for this actual feeder application are shown in Fig. 8. It can be seen that the feeder limit is not exceeded when considering the actual LTE curve. The energy-area for this actual energy curve calculates to 1902 MA²·s·km. If the instantaneous curve was not applied at the B-end, the conductor limit would have been exceeded for 2 km from 98 to 100 km's. The energy-area calculates to 3673 MA²·s·km. The application of the instantaneous curve half's the potential energy-area. It is not shown in Fig. 8, but from a LTE evaluation perspective the feeder can be set to initiate an ARC cycle as the exposure would still be below the conductor limit.

6. Philosophy and setting considerations

When setting the protection in a network, guidance should be taken from the protection philosophy that is to be applied to the feeder protection elements. This philosophy provides guidance in terms of speed, selectivity, sensitivity, dependability and security [35]. In [36] HV feeders are evaluated to determine if conductor damage can occur based on a general HV protection philosophy. This philosophy evaluated is extended to the setting of the main impedance (as a step distance application) and the back-up protection. The zone 1, 2 and 3 elements were set with different reach settings and increasing time delays. The current based back-up protection is set to pick-up above load and grade with the main and downstream protection. The LTE evaluation concept as introduced here is applied in evaluating the general protection philosophy to show how the philosophy is meeting and failing the set damage criteria. The philosophy was applied to a large number of actual feeders with their actual fault currents and the conclusion was that the main protection philosophy is adequate and LTE analysis is required for back-up protection (based on the applied philosophy).

7. Conclusion

In the busbar fault level analysis it was shown that the fault levels are high enough to damage conductors. This is as a result of LTE exposure in an HV network. LTE is influenced by the magnitude and the duration of this fault current. Fast fault clearing is critical in reducing the LTE exposure, but the maximum LTE exposure position does not necessarily coincide with the longest fault exposure time. Reducing the fault clearing time can be achieved by applying an instantaneous curve, reducing the TM on IDMT elements and ensuring that the ratio of fault current to pick-up current is sizeable (greater than one). It was shown that for multisource feeders it is not only the number of ARC attempts that influence the LTE but also the dead time setting on the ARC element. With multiple sources present on a feeder the complexity of the LTE calculation increase when compared to a radial feeder application. The traditional form of the IDMT equation cannot be used for interconnected networks as the measured RMS fault current through the relay may change before a trip command is sent to the CB. A new average disc speed IDMT relay model was developed to calculate the expected trip time of the relays. This LTE analysis should also be applied to evaluate the effect of earth faults on conductors in HV networks.

8. Acknowledgments

The authors acknowledge the assistance that was received from Eskom Holdings SOC Limited and the University of Pretoria in the writing of this article.

9. References

[1] IEEE Std. 141: 'IEEE Recommended Practice for Electric Power Distribution for Industrial Plants', 1994.
[2] RSA Grid Code Secretariat. (2014, July). RSA Distribution Code Definitions Ver. 6, NERSA, South Africa, [Online]. Available: http://www.nersa.org.za
[3] Gönen, T.: 'System Protection', in: 'Modern Power System Analysis' (New York, Wiley & Sons, Inc, USA, 1988, 1st ed.), pp. 339 -429.
[4] Warrington, A.R.C.: 'Overcurrent Protection', in (vol. 1): 'Protective relays – their theory and practice' (Fletcher & Son Ltd, Norwich, Great Britain, 1968, 2nd ed.), pp. 1 -17, pp. 141 -167.
[5] The Electricity Council: 'The application of protection to transmission systems', in (vol. 3): Power System Protection (The Institution of Electrical Engineers, London, UK, 1997, 2nd ed.), chap. 17.
[6] Tan, J.C., McLaren, P.G., Jayasinghe, R.P., et al.: 'Software model for inverse time overcurrent relays incorporating IEC and IEEE standard curves'. IEEE

Canadian Conference on Electrical and Computer Engineering (CCECE), 2002, pp. 37–41.
[7] Keil, T. and Jager, J.: 'Advanced coordination method for overcurrent protection relays using nonstandard tripping characteristics', IEEE Trans. Power Del., Jan. 2008, 23, (1), pp. 52 -57.
[8] IEEE Std. C37.230: 'IEEE Guide for protective relay applications to distribution lines', 2007.
[9] Mason, C.R.: 'Line protection with overcurrent relays', in: 'The art and Science of Protective Relaying' (Wiley, New York, 1956), pp. 259 -295.
[10] AREVA T&D: 'Network Protection and Automation Guide' (AREVA T&D, Stafford, UK, 2011), chap. 2, 9, 10 and 14.
[11] Mousavi, S.M., Askarian Abyaneh, H., and Mahdavi, M.: 'Optimum setting and coordination of overcurrent relays considering cable damage curve'. IEEE PowerTech, Bucharest, June 28 -July 2, 2009, pp. 1 -5.
[12] Smith, T. and Hunt, R: 'Current transformer saturation effects on coordinating time interval', IEEE Trans. Ind. Appl., 2013, 49, (2), pp. 825 -831.
[13] Slabbert, M.J., Naidoo, R., Bansal, R.C., et al.: 'Evaluating phase over-current protection philosophies for medium-voltage feeders applying let-through energy and voltage dip minimization', Electric Power Components and Systems, 2016, 44, (2), pp. 206-218.
[14] Mitolo, M., and Tartaglia, M.: 'An analytical evaluation of the factor k^2 for protective conductors', IEEE Trans. Ind. Appl., 2012, 48, (1), pp. 211-217.
[15] Parise, G., and Adduce, M.: 'Conductor protection against short circuit current: available $I^{*2}t$ evaluation'. IEEE Industry Applications Conference, St. Louis, MO, USA, Oct. 1998, pp. 2336 -2341.
[16] Callister, W.D., Jr.: 'Mechanical properties of metals', in: 'Materials science and engineering an introduction' (New York, Wiley & Sons, Inc, USA, 2003, 6th ed.), chap. 2 and 6.
[17] Wareing, B.: 'Conductor characteristics and selection', in (vol. 48): 'Wood Pole Overhead Lines' (London, United Kingdom: The Institution of Engineering and Technology, 2008, 1st ed.), pp. 114–140.
[18] Bello, M. M., 'Network planning guideline for lines and cables', Eskom, Johannesburg, South Africa, DGL 34-619, Nov. 2010.
[19] Kussy, F.W, and Warren, J.L.: 'Effects of short-circuit currents on conductors', in: 'Design Fundamentals for Low-Voltage Distribution and Control' (New York, Marcel Dekker Inc., USA, 1987, 1st ed.), pp. 119-131.
[20] Tartaglia, M., and Mitolo, M.: 'An analytical evaluation of the prospective I^2t to assess short-circuit capabilities of cables and busways', IEEE Trans. Power Del., 2010, 25, (3), pp. 1334 -1339.
[21] Thomas, E.S.: 'Bonding requirements for conductive poles'. IEEE Rural Electric Power Conference (REPC), April 2012, pp. A4-1-A4-6.
[22] Olejnik, B.: 'Selected protective algorithms of modern IED', Computer Applications in Electrical Engineering, 2013, 11, pp. 389 -395.
[23] Goh, Y.L., Ramasamy, A.K., Abidin, A.A.Z., et al.: 'Modelling of Overcurrent Relay Using Digital Signal Processor'. Proc. IEEE Symposium on Industrial Electronics and Applications (ISIEA), Penang, Malaysia, 2010, pp. 367 -370.
[24] IEEE Std. C37.104: 'IEEE Guide for automatic reclosing of line circuit breakers for AC distribution and transmission lines', 2002.
[25] Eskom Holdings SOC Limited, 'Eskom Integrated Report 2016', Eskom Holdings SOC Limited, Johannesburg, South Africa, 31 March 2016.
[26] Spoelstra, J., 'Eskom Transmission System 2015-2016 Annual Fault Level Report Rev. 1', Eskom Holdings SOC Limited, Johannesburg, South Africa, Rep. 240-118802871, 31 Oct. 2016.
[27] Schmidt, H., and Speckhofer, G.: 'Experimental and Theoretical Investigation of High-Pressure Arcs-Part I: The Cylindrical Arc Column (Two-Dimensional Modeling)', IEEE Trans. Plasma. Sci., Aug. 1996, 24, (4), pp. 1229 -1238.
[28] Nasser, E.: 'Some physical properties of electrical discharges on contaminated surfaces', IEEE Trans. Power. App. Syst., April 1986, PAS-87, (4), pp. 957 -963.
[29] Arrayas, M., and Trueba, J.L.: 'Investigations of pre-breakdown phenomena: streamer discharges', Contemporary Physics, July -Aug. 2005, 46, (4), pp. 265 -276.
[30] Sidhu, T.S., Sachdev, M.S., and Wood, H.C.: 'Design of a Microprocessor-Based Overcurrent Relay'. Proc. IEEE Western Canada Conference on Computer, Power and Communications Systems in a Rural Environment (WESCANEX '91), 1991, pp. 41 -46.
[31] IEEE Std. C37.112: 'IEEE Standard Inverse-Time Characteristic Equations for Overcurrent Relays', 1996.
[32] Schweitzer, E.O., and Zocholl, S.E.: 'The Universal Overcurrent Relay', IEEE Ind. Appl. Mag., May/June 1996, 2, (3), pp. 28 -34.
[33] Sorrentino, E.: 'Behaviour of induction disc overcurrent relays as a function of the frequency', Electric Power Systems Research, Feb. 2017, 143, pp. 474 -481.
[34] IEEE Std. C57.109: 'IEEE Guide for Liquid-Immersed Transformer Through-Fault-Current Duration', 1993.
[35] Slabbert, M.J., Naidoo, R., Bansal, R.C..: Medium voltage phase overcurrent feeder protection, in Power System Protection in Smart Grid Environment, R.C. Bansal (Editor), CRC Press, book scheduled for publication in 2018.
[36] Slabbert, M.J., Naidoo, R., Bansal, R.C.: The application of let-through energy protection to the main and back-up protection elements on high voltage overhead feeders'. CIGRE 2018, Paris, France, 26-31 Aug. 2018.